
Original Paper

A Second Order Exact Scaling Method for Turbomachinery Performance Prediction

Peter Fanz Pelz and Stefan Sebastian Stonjek

Chair of Fluid Systems Technology, Technische Universität Darmstadt
Magdalenenstr. 4, Darmstadt, 64289, Germany
peter.pelz@fst.tu-darmstadt.de, stefan.stonjek@fst.tu-darmstadt.de

Abstract

A scaling method valid for most turbomachines based on first principles is derived. It accounts for axial and centrifugal turbomachines with respect to relative gap width / tip clearance, relative roughness, Reynolds number and/or Mach number for design and off-design operation as well. The scaling method has been successfully validated by a variety of experimental data obtained at TU Darmstadt. The physically based, hence reliable and universal method is compared with previous, empirical scaling methods.

Keywords: Scaling, Efficiency, Axial, Centrifugal, Turbine, Compressor, Fan, Reynolds number, Mach number, Size, Tip Clearance, Gap, Roughness

1. Introduction

The value and acceptance of a turbomachine is not only determined by pressure characteristics but mainly by efficiency. In general the performance characteristic of a turbomachine changes if the following physical quantities are varied: Machine size, given by the impeller diameter D , angular speed $\Omega = 2\pi n$, kinematic viscosity ν , density ρ , compressibility measured by the speed of sound a , typical roughness height K , gap width (centrifugal: gap between shroud and inlet) or tip clearance S (axial) and *shape* of the machine.

The performance is characterized by efficiency $\eta = \eta(\dot{V}, \Omega, D, \nu, \rho, a, K, S, \text{shape})$ and specific work $Y = Y(\dot{V}, \Omega, D, \nu, \rho, a, K, S, \text{shape})$. The shape of the machine is described by a finite number of dimensionless parameters, such as the ratio of chord length to the impeller diameter $\kappa_l = l/D$. By means of dimension analysis the number of independent parameters can be reduced by 3. This yields to the dimensionless products flow coefficient $\varphi = 4\dot{V}/uD^2\pi$ with the circumferential speed given by $u = \Omega D/2$, Reynolds number $Re = uD/\nu$, Mach number $Ma = u/a$, relative roughness $k = K/L$ with the characteristic length L , relative gap width or tip clearance $s = S/L$, efficiency $\eta = 1 - P_{\text{loss}}/P_{\text{shaft}}$ wherein P_{shaft} is the shaft power and P_{loss} the sum of dissipative losses and pressure coefficient $\psi = 2Y/u^2$.

Scaling methods serve to predict the changing in efficiency $\eta = \eta(\varphi, Re, Ma, k, s, \text{shape})$ and pressure coefficient $\psi = \psi(\varphi, Re, Ma, k, s, \text{shape})$ depending on variation of one or more of the listed dimensionless parameters for the same volume flow φ and same machine shape. Hence the scaling method gives an answer to the question: What is the difference in efficiency between model (subscript m) and full scale machine?

$$\eta(\varphi, Re, Ma, k, s, \text{shape}) - \eta(\varphi, Re_m, Ma_m, k_m, s_m, \text{shape}) = ?$$

The first physically based scaling method can be traced back to Pfleiderer in the year 1946 [1]. He was guided by the thought, that the inefficiency $\varepsilon = 1 - \eta$ is proportional to the friction coefficient c_f . For hydraulically smooth surface with $c_f \sim Re^\alpha$ the ratio of inefficiencies from full scale machine to model yields

$$\frac{1 - \eta}{1 - \eta_m} = \left(\frac{Re}{Re_m}\right)^\alpha \quad (1)$$

According to pipe flow analogy with turbulent flow and hydraulically smooth wall α was set to $-0.25 \dots -0.1$. Ackeret in 1948 improved the method of Pfleiderer, by taking inertia losses into account (published by Mühlemann [2])

$$\frac{1 - \eta}{1 - \eta_m} = V \left[1 + \left(\frac{Re}{Re_m} \right)^\alpha \right], \quad (2)$$

where the loss distribution factor V was arbitrarily set to $1/2$. Heß and Pelz [3] considered the loss distribution factor depending on the flow coefficient $V(\varphi)$. This considers the increase of inertia losses at off design operation.

Casey and Robinson [4] published an empirical scaling method where the difference in efficiency is given by

$$\Delta\eta = \eta - \eta_m = -B_{\text{ref}}(\sigma) \frac{\Delta c_f}{c_{f,\text{ref}}}. \quad (3)$$

B_{ref} is an empirically determined function of specific speed σ . They claimed the validity for all types of turbomachinery regardless of fans and compressors, although the Mach number is not considered in Eq. 3. Both Eq. 2 and Eq. 3 need empirical functions which are machine dependent. Hence there is always an uncertainty in applying these methods.

It is possible to yield a scaling method by means of total derivative of the inefficiency $\varepsilon \stackrel{\text{def}}{=} 1 - \eta$. Taking only terms of first order in inefficiency into account [5], [6], yields to

$$\Delta\eta = -\varepsilon(\sigma, Re_m, Ma_m, k_m, s_m, \text{shape}) \frac{\Delta c_f}{c_{f,m}}. \quad (4)$$

Comparing the methods Eq. 3 and 4 it is obvious that the empirical function $B_{\text{ref}}(\sigma)$ is similar to the inefficiency $\varepsilon(\text{type, size, quality})$, where the machine *type* is given by the specific speed, the *size* by Mach and Reynolds number and the *quality* by relative roughness, gap width and shape.

The task of this work is (i) to further improve the method Eq. 4 to account for second order terms $\sigma(\varepsilon^2)$ and for tip clearance / gap losses as well and (ii) to omit any empirical relations as far as possible to gain a universal and physically based scaling method.

2. Second Order Scaling Method

2.1 Logarithmic Change of Inefficiency

The specific mechanical power $w_{\text{shaft}} = P_{\text{shaft}}/\dot{m}$ transmitted through the shaft of the machine is equal to the enthalpy increase

$$w_{\text{shaft}} = h_{t2} - h_{t1}, \quad (5)$$

assuming there is no heat exchange with the environment [7] and the process is stationary in average of time [8]. The change of inner energy from 1 to 2 is equal to the loss of enthalpy h_{loss} . The ratio of enthalpy loss and specific mechanical power is the inefficiency

$$\varepsilon \stackrel{\text{def}}{=} 1 - \eta = \frac{h_{\text{loss}}}{w_{\text{shaft}}}. \quad (6)$$

Both, the enthalpy loss and the shaft power can be described in dimensionless way. The dimensionless measure of the shaft power is the power coefficient. For turbomachinery under compressible conditions the power coefficient is defined by

$$\lambda \stackrel{\text{def}}{=} \frac{2w_{\text{shaft}}}{u^2}. \quad (7)$$

Contrary under incompressible conditions e. g. with fans it is defined by

$$\Lambda \stackrel{\text{def}}{=} \frac{2P_{\text{shaft}}}{\rho u^3 A_{\text{ref}}} = \lambda \varphi \quad (8)$$

with $A_{\text{ref}} = \pi D^2/4$. For the definition of the drag coefficient the enthalpy loss is made dimensionless by dividing through the square of circumferential speed

$$c_d \stackrel{\text{def}}{=} \frac{2h_{\text{loss}}}{u^2}. \quad (9)$$

Often the drag coefficient is defined by the relative inlet velocity $w^2 \approx u^2(1 + \varphi^2)$. Both definitions are equivalent by the transformation

$$c_{d,w} \stackrel{\text{def}}{=} \frac{2h_{\text{loss}}}{w^2} = c_d / (1 + \varphi^2). \quad (10)$$

For compactness we use c_d and can write

$$\varepsilon \stackrel{\text{def}}{=} 1 - \eta = \frac{c_d}{\lambda} . \quad (11)$$

To end up with a scaling method we take the logarithmic change of Eq. 11 and get the general valid equation, which will be the basis for the new scaling method:

$$\frac{d\varepsilon}{\varepsilon} = \frac{dc_d}{c_d} - \frac{d\lambda}{\lambda} . \quad (12)$$

Since $c_d = \varepsilon\lambda$ Eq. 12 is equivalent to

$$d\varepsilon = \varepsilon \frac{dc_d}{c_d} - \varepsilon^2 \frac{d\lambda}{c_d} , \quad \text{or} \quad d\eta = -\varepsilon \frac{dc_d}{c_d} + \sigma(\varepsilon^2) . \quad (13)$$

Regarding both terms on the right hand side, we denote that a second order scaling method, which is in focus of this paper. Neglecting the term of order ε^2 in Eq. 13 and comparing it with Eq. 3 yield $B_{\text{ref}} = c_{f,\text{ref}}/\lambda$ for the method of Casey and Robinson [4].

2.2 Froude's Assumption

William Froude (1810-1879) was a British naval engineer and today his method of studying the resistance of ships is generally adopted. The so called Froude's assumption is the following: Losses (inertia drag, surface friction resistance and wave drag) are independent of each other:

$$c_d = c_i(s, \psi, \varphi) + c_f(Re, k, \varphi) + c_w(Ma, \varphi, \text{shape}) . \quad (14)$$

In a similar way the power coefficient can be decomposed into the power transferred to the fluid within the blade channel (subscript *Euler*), the power needed to have the internal leakage flow circulating (subscript *l*), and the power needed to get over the fluid friction at the discs (subscript *d*) outside the blade channel (where we assume a low Mach number flow):

$$\lambda = \lambda_{\text{Euler}}(\varphi) + \lambda_l(s, \psi, \varphi) + \lambda_d(Re, k, \varphi) . \quad (15)$$

There are two important limiting cases concerning the Mach number in turbomachines. (i) with fans or hydraulic machines fulfilling the condition $Ma^2 \ll 1$ [5], wave losses are negligible. (ii) with turbomachines that run at high Mach numbers like compressors and turbines ($Ma^2 \approx 1$) the influence of Reynolds number vanishes and wave losses become dominant. For that case it counts $c_w \gg c_f$ and therefore $c_d \approx c_i(s, \psi, \varphi) + c_w(Ma, \varphi, \text{shape})$.

The application of our method to measured data has shown better results using a friction (subscript *f*) or wave (subscript *w*) drag coefficient $c_d \approx c_{f,w}$ at the best efficiency point (BEP), i. e. neglecting inertia losses only at that operation point, instead of using the calculated value of $c_d = \varepsilon\lambda$ where ε and λ are measured values in each case. This is due to measurement uncertainties but for specific purposes it might be useful to apply the exact relation. Since $d\lambda_{\text{Euler}} \equiv 0$ the logarithmic change of inefficiency Eq. 12 using Froude's assumption reads

$$\frac{d\varepsilon}{\varepsilon} = \frac{dc_d}{\varepsilon\lambda} - \frac{d\lambda}{\lambda} \approx \frac{dc_i + dc_{f,w}}{c_{f,w}} - \frac{d\lambda_l + d\lambda_d}{\lambda} \quad \text{at BEP} . \quad (16)$$

2.3 Axial and Centrifugal Machines scaled at Best Efficiency Point (BEP)

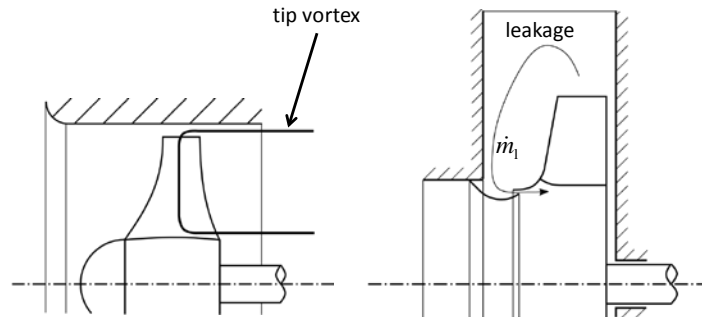


Fig. 1 Different gap loss mechanisms in axial (left) and centrifugal (right) machines.

The physics of tip clearance flow in unshrouded machines, e. g. axial or diagonal, is quite different from the situation for shrouded machine (Fig. 1). Recently Pelz and Karstadt [9] developed a well validated model for axial machines with $d\lambda_d \equiv 0$ and

$d\lambda_1/\lambda \ll dc_{\text{induced}}/c_d$, with the induced drag given by

$$c_i - c_{i0} = c_{\text{induced}} = C s \lambda^2. \quad (17)$$

C is a machine typical, shape dependent but dimensionless constant and s the relative tip clearance S/D . Hence the scaling method Eq. 16 reads

$$\frac{d\varepsilon}{\varepsilon} = \frac{dc_{f,w}}{c_{f,w}} + \Theta \frac{ds}{\varepsilon \lambda} \quad (18)$$

$$\text{at BEP with the abbreviate } \Theta = \begin{cases} C \lambda^2 & \text{unshrouded machine} \\ 4\mu d_s \psi^{\frac{3}{2}}/\varphi & \text{shrouded machine} \end{cases}.$$

For shrouded blades typical for centrifugal machines, the leakage flow contributes to both, the power coefficient and the loss coefficient in Eq. 16 due to mixing losses. The Appendix of this paper gives the derivation of Θ for shrouded machines. μ is the discharge coefficient and $d_s = D_s/D$ the relative diameter of the gap.

2.4 Wave and Friction Losses

A model for the frictional drag coefficient $c_f(Re, \varphi, k)$ and wave drag coefficient $c_w(Ma, \varphi, \text{shape})$ in the second order scaling formula Eq. 18 is pending at this point. A flow along a flat plate can serve as a model for the flow through blade channel to gain the frictional drag coefficient. This is not possible for the wave drag, since the waves (Prandtl Meyer or shock waves) within the machine depend strongly on the machine shape, i.e. the dimensionless ratios of length $\kappa_1, \dots, \kappa_N$. The discussed limiting case $c_d(Ma \approx 1, Re) = c_d(Ma)$ is confirmed by measurements done by Miller and Bailey [10].

Changing the rotational speed of the (model) machine will increase both Mach number and Reynolds number, since $Ma \sim nD$ and $Re \sim nD^2$. But supposed the wall friction model is sufficiently accurate and inertia losses are negligible at BEP the Mach number influence can be extracted from the measured machine efficiency. In the context of scaling frictional losses the model of a flow along a flat plate is sufficient to predict the frictional drag coefficient of a turbomachine. We use the Reynolds number calculated with the relative velocity at outlet

$$Re_p = \frac{l}{D} \frac{1}{1 - v^2} \frac{1}{\sin \beta_0} \varphi Re \quad (19)$$

for axial and

$$Re_p = \frac{1}{4} \frac{l}{b_2} \frac{1}{\sin \beta_0} \varphi Re \quad (20)$$

for centrifugal machines. v is the hub-tip ratio and β_0 the design stagger angle. For $k \leq 100/Re_p$ the wall surface is hydraulically smooth and

$$c_f = 0.455 (\log_{10} Re_p)^{-2.58} \quad (21)$$

is a good approximation for the frictional drag coefficient [11]. For $k > 100/Re_p$ the wall is hydraulically rough and

$$c_f = (1.89 - 1.62 \log_{10} k)^{-2.5} \quad (22)$$

should be used.

3. Scaling Off-Design Operation – The Master Curve Approach

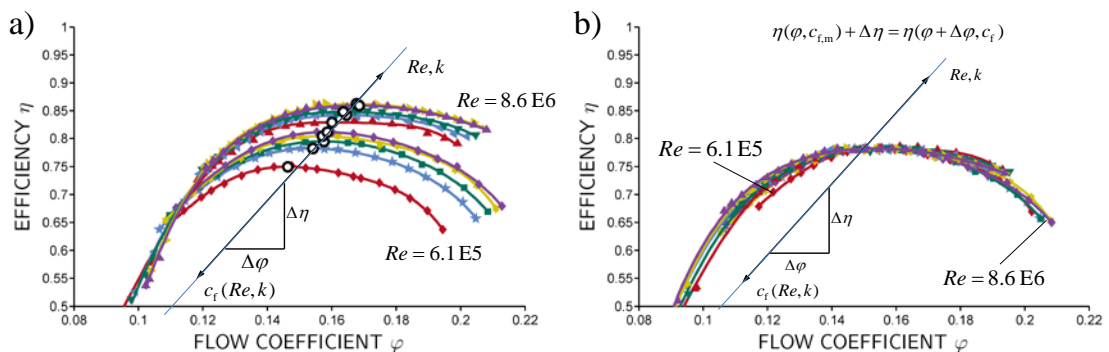


Fig. 2 Performance characteristics of axial fans of specific speed $\sigma = 1.46$ tested at the Chair of Fluid Systems Technology,

TU Darmstadt, with the stagger angle $\Delta\beta_0 = -6^\circ$. a) efficiency variation with Reynolds number, b) master curve.

Fig. 2a shows the dependency of efficiency versus flow coefficient for a typical axial fan at different Reynolds numbers [12]. The Reynolds number differs from 6.1E5 to 8.6E6. The markers (black unfilled dots) designate the peak efficiency points. For a detailed fan description see Heß [12]. It is obviously for this and all other measurements, not matter if axial or centrifugal fan, that the peak efficiency points are all aligned along one straight line. If we shift the measured efficiency curves along that straight line, we end up with one single curve which we call *master efficiency curve of the turbomachine* (see Fig. 2b). If a machine does have a master curve, the condition

$$\eta(\varphi, c_m) + \Delta\eta = \eta(\varphi + \Delta\varphi, c), \text{ with } \Delta\eta \sim \Delta\varphi \quad (23)$$

is fulfilled. The subscript m stands for model or reference and c is the loss coefficient. The subscript f,w has been omitted for shortness reasons. Even though we give Eq. 23 here for completeness it is important to mention, that our visible impression by comparing Fig. 2a and Fig. 2b is much more convincing than arguing with an equation like Eq. 23.

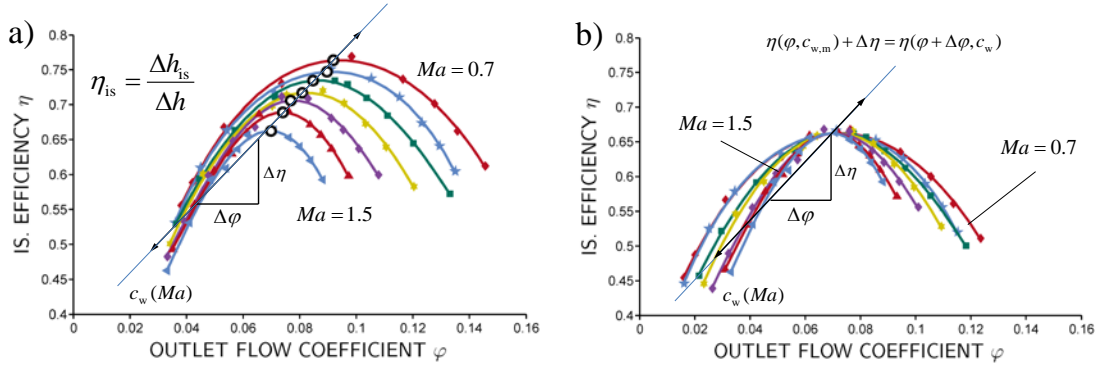


Fig. 3 Performance characteristics of a compressor of a turbo charger without influence of heat transfer [7]. a) efficiency variation with Mach number, b) master curve.

Eq. 23 holds for all efficiency curves measured at our own laboratory for different specific speeds i.e. for pumps, fans or compressors, axial or centrifugal. A further example is given by Fig. 3, which shows the dependency of efficiency versus flow coefficient for a compressor of a turbocharger at different Mach numbers. Isentropic efficiency is defined by the ratio of isentropic enthalpy difference and real enthalpy difference $\eta_{is} = \Delta h_{is} / \Delta h$. The Mach number differs from 0.7 to 1.5. In this case, the effect of Mach number dominates the characteristic but Eq. 23 is still fulfilled.

4. Scaling the Flow Coefficient φ

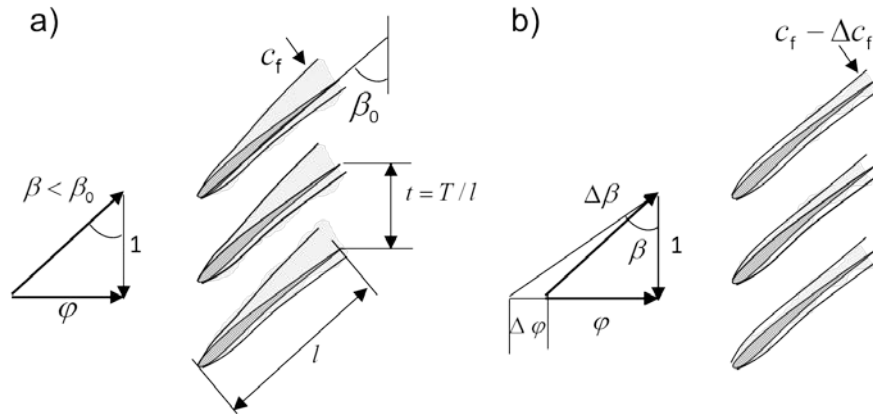


Fig. 4 Uneven boundary layers on pressure and suction side. The difference between a) and b) cascade is the Reynolds number and hence the boundary layer thickness.

In this section we describe the physical reason for the proportional relation $\Delta\eta \sim \Delta\varphi$ in a short form and give an analytic equation for it. A more detailed description can be found in [6]. We start the discussion with a schematic sketch of the flow through a blade cascade. Fig. 4a shows the flow through a blade cascade with small Reynolds number. The Reynolds number and the relative roughness k determine the boundary layer thicknesses $\delta_+ = \delta/l$ and hence the fluid displacement and momentum losses. In the context of the current considerations, it is sufficient and more over very convenient to use the relation

$$\delta_+ \sim c_f = c_f(Re, k) . \quad (24)$$

Fig. 4b shows schematically the geometric similar machine at a higher Reynolds number. As usual all velocities are measured in multiplies of the circumferential speed u , the length of the adjacent side of the velocity triangle is one and the opposite side is given by the flow coefficient $\varphi = c_m/u$ (here c_m is the absolute meridional velocity component). Increasing the rotational

speed or machine size will result in a thinning of the boundary layer. To achieve the optimal flow angle in the right cascade the flow coefficient φ has to be changed to $\varphi + \Delta\varphi$ [6]. Here the different response from suction to pressure side to a change in Reynolds number is important. The relative change on the suction side is much bigger than on the pressure side which is clarified by the classical work of Schlichting and Scholz published in the year 1950 [13]. The change of the peak efficiency point for small changes is given in [6] by

$$\Delta\varphi = -\frac{1}{\hat{C}(t, \beta_0)} \Delta c_f \quad (25)$$

with

$$\hat{C}(t, \beta_0) = \frac{t}{2} (\sin \beta_0 + \cos \beta_0) \quad (26)$$

wherein t is the dimensionless blade spacing of the blade cascade. Eq. 26 was derived without considering the pressure gradient in the blade channel. It results from a cascade of plates with simplifications in displacement thickness calculation. Hence the determination of the constant with Eq. 26 overestimates the value of \hat{C} clearly. We got a constant value of approximately 0.25 for all our fans from measurements no matter if the fans are centrifugal or axial.

5. Validation of the Method

For application we replace the differential operator in Eq. 18 with differences and get

$$\Delta\eta = -(1 - \eta) \left[\frac{\Delta c_f}{c_f} + \theta \frac{\Delta s}{\varepsilon \lambda} \right] \quad (27)$$

The first term in the squared brackets accounts for the change in efficiency due to Reynolds and roughness effects. It is validated with test data from two axial fans with a diameter of 1000 mm, 250 mm and two centrifugal fans with 2240 mm, 896 mm diameter [12], [14]. Except Reynolds number, Mach number and relative roughness the two axial and centrifugal fans are similar to each other.

The second term in Eq. 27 considers the change in tip clearance or gap width from model to full scale machine. The tip clearance of the axial fan was altered by reducing the blade length [12]. Additionally two centrifugal pumps with a diameter of 260 mm and 350 mm analyzed in [15] and [16] are examined, because there is no test data for the centrifugal fan with altered gap width at the moment.

The test stands are built and measurements of the performance characteristics are evaluated complying with ISO 5801 standard [17]. The shaft power of the fans is measured by a flying mount torque metering shaft without measuring any mechanical losses in bearings and gaskets. The variation of the Reynolds number within one machine is achieved by changing the rotational speed. The test data of the lowest Reynolds number has an uncertainty below 2.3 % points of total efficiency due to accuracy of torque measurement. The uncertainty of test data with highest Reynolds number is quite lower (below 0.5 % points).

We will validate the two terms of Eq. 27 separately in the following. Figure 5 shows measured performance characteristics from centrifugal fan and predicted characteristics using different scaling methods mentioned in introduction ($\Delta s = 0$). The scaling is performed with test data from the large model machine (lm) represented by open dots. The desired characteristic is the test data of the full scale machine (fs) represented by black dots. The predicted performance characteristic using the new method (Pelz and Stonjek) shows the best agreement to measured data.

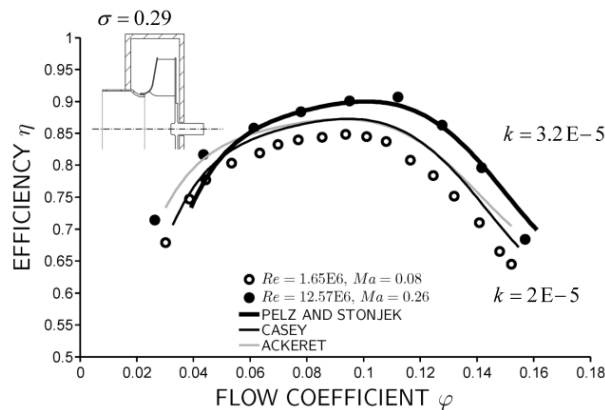


Fig. 5 Characteristic of the centrifugal fan with $\sigma = 0.29$ scaled up with different methods.

Figure 6 shows the scaling of the gap width for two centrifugal pumps with a common value for μ of 0.7 for both pumps ($\Delta c_f = 0$). The method has been applied to the test data of design gap width represented by open dots and the desired characteristic is the test data with altered gap width represented by black dots.

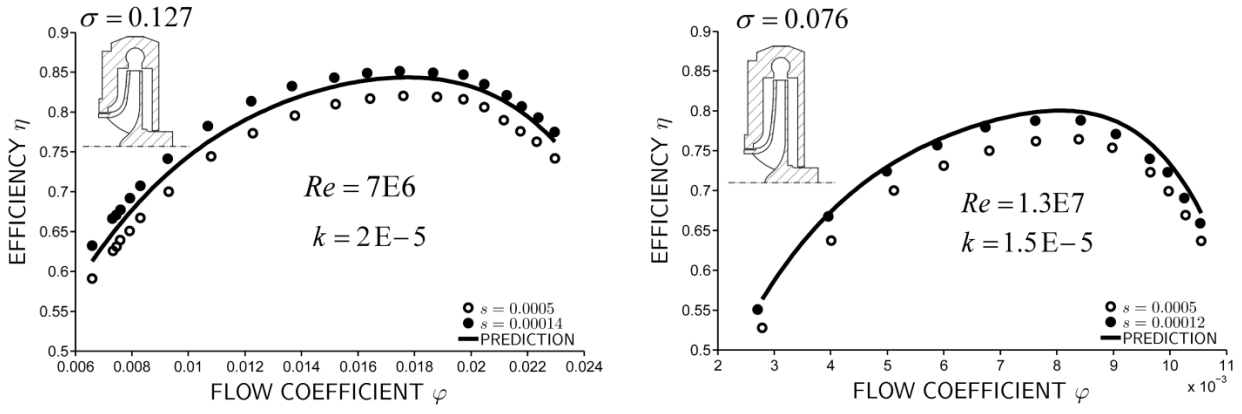


Fig. 6 Centrifugal pumps with changed gap width. The specific speed of the pump on the left side is $\sigma = 0.127$ [15] and on the right side $\sigma = 0.076$ [16].

While the efficiency of the pump on the left in Fig. 6 is slightly underestimated, it is overestimated for the second pump on the right. The reason is the uncertainty in μ in Eq. 18 due to a changed swirl in the volute before gap entrance. This is caused by another rotor diameter from the pump on the left compared to the pump on the right.

Figures 7 and 8 show the measured data and the predicted performance characteristics of the axial fans ($\Delta s = 0$). The scaling is performed with the test data of lowest Reynolds number of the small model machine (sm) (open dots) and the desired characteristic is the test data of the highest Reynolds number of the large model machine (lm) (black dots). To obtain different geometries on the same test rig, the stagger angle of the axial fan was varied. β_0 is the stagger angle of the design point. It was varied from $\Delta\beta_0 = +6^\circ$ to $\Delta\beta_0 = -12^\circ$. The prediction of the characteristic with the method introduced in this work is good for small variations from design point stagger angle. The low stagger angle of $\Delta\beta_0 = -12^\circ$ results in significant deviations between measurement and predictions regardless of used scaling method. The original Ackeret formula shows the worst prediction for our test cases.

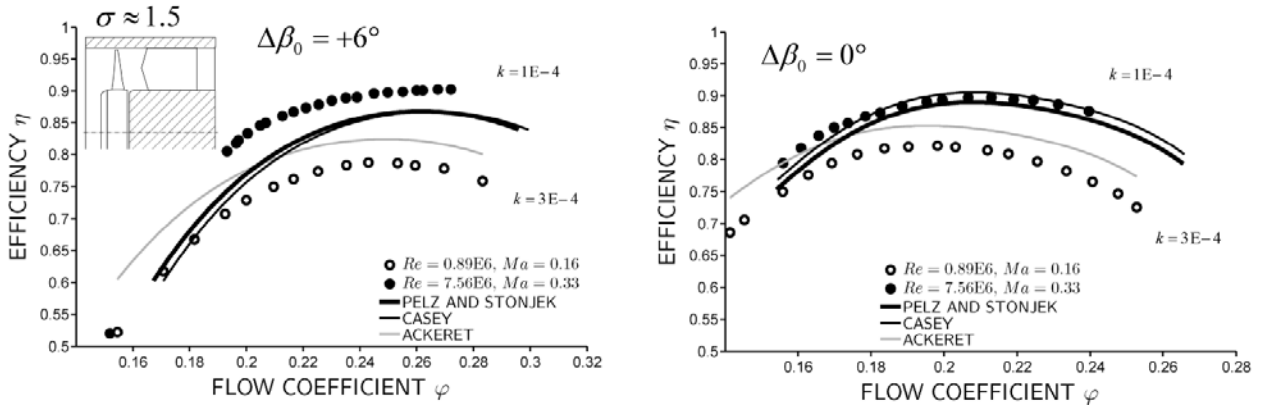


Fig. 7 Axial fan with stagger angle $\Delta\beta_0 = +6^\circ$ ($\sigma = 1.64$) and $\Delta\beta_0 = 0^\circ$ ($\sigma = 1.49$).

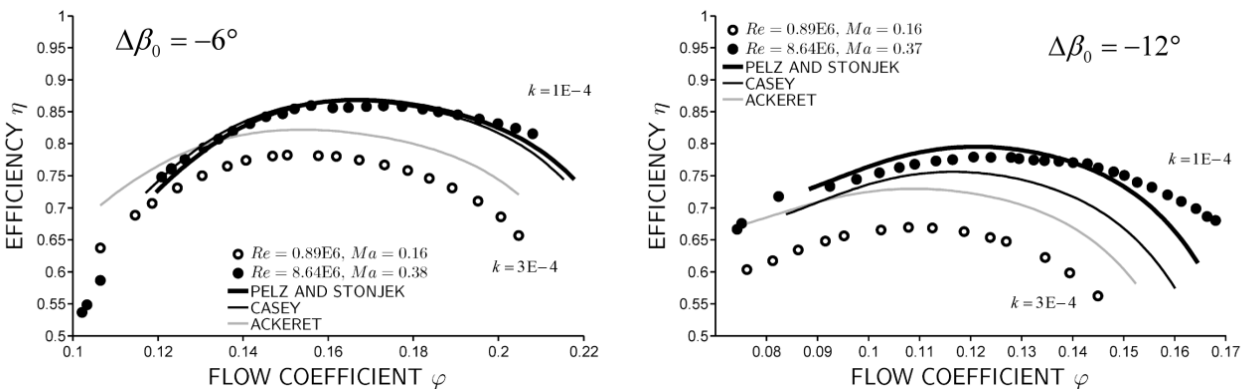


Fig. 8 Axial fan with stagger angle $\Delta\beta_0 = -6^\circ$ ($\sigma = 1.46$) and $\Delta\beta_0 = -12^\circ$ ($\sigma = 1.53$).

For the validation of the right part of Eq. 27 the tip clearance from the same axial fan was changed from 0.1 % to 0.5% with the same stagger angles as above. Figure 9 and 10 show the test data (black dots: desired characteristic) and the predicted efficiency curve calculated by Eq. 27 at a fixed Reynolds number of $5.4E6$ ($\Delta c_f = 0$).

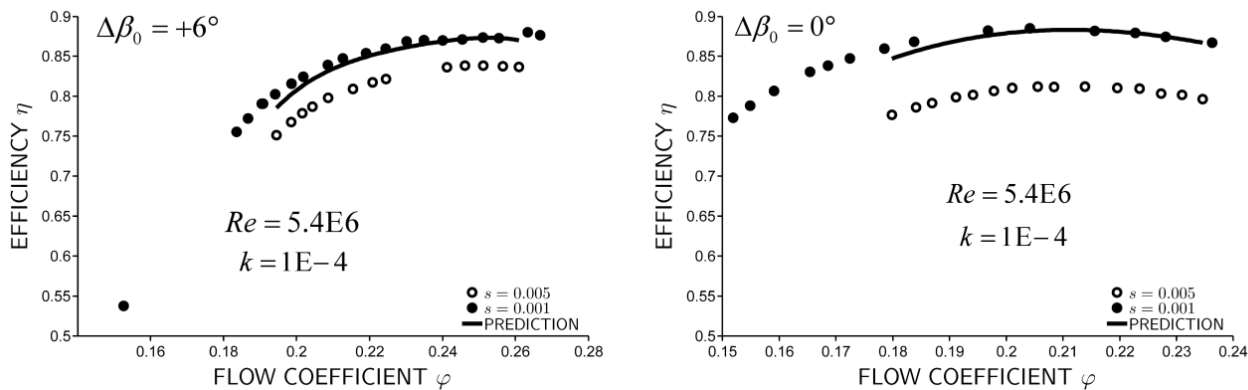


Fig. 9 Tip clearance loss validation for the axial fan with stagger angle $\Delta\beta_0 = +6^\circ$ ($\sigma = 1.64$) and $\Delta\beta_0 = 0^\circ$ ($\sigma = 1.49$).

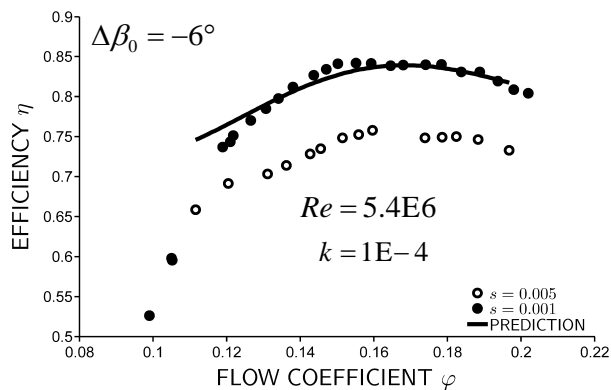


Fig. 10 Tip clearance loss validation for the axial fan with stagger angle $\Delta\beta_0 = -6^\circ$ ($\sigma = 1.46$).

The predicted efficiency curve fits the measured data with small deviations.

6. Conclusion

A new method for scaling up the efficiency of fans has been introduced in this work. The method has essential advantages compared to previous introduced scaling methods

- simple application,
- physical motivation for the scaling effect and the shift in flow rate,
- only one free parameter,
- scaling of Reynolds number, roughness and tip clearance / gap losses combined in only one formula and
- good results.

The method takes altered tip clearance / gap width in model and full scale machine into account. More work has to be done regarding to the determination of the constant for the shift in flow rate. Furthermore, especially for centrifugal fans scaling of disc friction losses could be necessary. This can be achieved by Eq. 39 in Appendix, where disc friction losses are not neglected. Nevertheless, the method shows good agreement to test data within the scope of the analyzed fans at the Chair of Fluid Systems Technology.

Acknowledgments

The authors would like to thank the Arbeitsgemeinschaft industrieller Forschungsvereinigungen "Otto von Guericke" e. V. (AiF), the Bundesministerium für Wirtschaft und Technologie (BMWi), and the Forschungsvereinigung für Luft- und Trocknungstechnik (FLT) e. V. whose support made this work possible. Additional thanks to the members of the supervising working group of the FLT, in particular to Mr. Christian Rohdich.

Nomenclature

Symbols

a	speed of sound [m/s]	h	enthalpy [Ws/kg]
A	area [m ²]	k	relative roughness
b	width [m]	K	absolute roughness height [m]
c_d	drag coefficient	l	chord length [m]
c_f	friction coefficient	L	characteristic length [m]
C, \hat{C}	constant	\dot{m}	mass flow rate [kg/s]
B_{ref}	scaling constant	Ma	Mach number
d	relative diameter	n	rotational speed [1/s]
D	diameter [m]	n_s	Schnelllaufzahl [1/s]

p	pressure [Pa]	α	Blasius constant
P	power [W]	β_0	design stagger angle
<i>quality</i>	quality	δ	specific diameter, boundary layer thickness [m]
r	radius (coordinate) [m]	δ_+	dimensionless boundary layer thickness
r_Ω	ratio of angular velocity	ε	inefficiency
Re	Reynolds number	η	efficiency
s	relative tip clearance / gap width	Θ	clearance constant
S	absolute tip clearance / gap width [m]	κ	ratio of lengths
<i>shape</i>	shape	λ	power coefficient (compressors)
<i>size</i>	size	Λ	power coefficient (fans)
<i>type</i>	type	μ	discharge factor
t	dimensionless blade spacing	ν	kinematic viscosity [m ² /s], hub tip ratio
T	blade spacing [m]	ρ	density [kg/m ³]
u	circumferential velocity [m/s]	σ	specific speed
w	specific power [Ws/kg]	τ	shear stress [Pa]
V	loss distribution factor	φ	flow coefficient
\dot{V}	volume flow rate [m ³ /s]	ψ	pressure coefficient
Y	specific work [Ws/kg]	Ω	angular velocity [1/s]

Indices

c	channel
d	disc
Euler	Euler
f	friction
i	inertia
is	isentropic
ideal	ideal
induced	induced
l	leakage
local	local
loss	loss
m	model
P	plate
ref	reference
remain	remaining
req	required
shaft	shaft
s	tip clearance / gap width
t	total
w	wave
0	design point
1	inlet
2	outlet

Appendix

Centrifugal Machine for Small Mach Number ($Ma \ll 1$)

Leakage. Contrary to axial machines the leakage flow driven by pressure difference between in- and outlet causes a high energetic flow back to the inlet (see Fig. 1).

The leakage flow in centrifugal machines is generally described by

$$\dot{m}_l = \mu A_s \sqrt{2\Delta p \rho} , \quad (28)$$

with the gap cross sectional area $A_s = 2\pi R_s S$ and the discharge factor μ [1]. The discharge factor depends on gap Reynolds number, type of sealing and pre swirl of the flow before entering the gap. For short cylindrical sealing gaps the in- and outflow losses dominate the gap resistance depending on Reynolds number [18].

On the one hand, the power consumption will rise with increasing leakage flow, on the other hand it is assumed, that the power, which is necessary to keep the leakage flow circulating, is dissipated completely. This assumption is justified concerning the mixing process of the high speed leakage flow and the low speed kernel flow in the inlet region.

The specific power loss through leakage flow is determined by

$$h_l \approx \frac{\dot{m}_l \Delta p}{\dot{m} \rho} . \quad (29)$$

Eq. 28 and Eq. 29 yield to the dimensionless power loss

$$c_{i,l} = \lambda_l = 4\mu\psi^{\frac{3}{2}} d_s \frac{1}{\varphi} \quad (30)$$

with the relative gap diameter $d_s = D_s/D$. As already mentioned μ depends on Reynolds number, but the main influence of the change in leakage flow is the relative gap width s and the driving pressure difference contained in ψ . The total derivative of Eq. 30 yields to

$$dc_{i,l} = d\lambda_l = 4\mu d_s \frac{1}{\varphi} \left(\frac{3}{2} s \psi^{\frac{1}{2}} d\psi + \psi^{\frac{3}{2}} ds \right) . \quad (31)$$

The influence of the change in pressure coefficient due to Reynolds effects is small compared to the influence of altering relative gap width from model to full scale machine. With $d\psi = 0$ we get

$$dc_{i,l} = d\lambda_l = 4\mu d_s \frac{1}{\varphi} \psi^{\frac{3}{2}} ds . \quad (32)$$

Disc friction. Following Pfleiderer [1] and other authors the specific disc friction power can be calculated by integrating the wall shear stress about the disc surface

$$h_d = \frac{\Omega}{\dot{m}} \int r \tau dA . \quad (33)$$

Assuming pipe friction analogy, which is suitable concerning the developed flow in the impeller side room chamber, the shear stress can be calculated by

$$\tau = \frac{1}{8} \rho c_{f,d,local} (1 - r_\Omega)^2 \Omega^2 r^2 , \quad (34)$$

where $c_{f,d,local}$ is the local friction coefficient, r_Ω the ratio of angular velocity of the rotating fluid kernel and r the radius of disc. With $r_\Omega \approx 1/2$ (rotating fluid kernel with half rotational speed than rotor, which is valid if the roughness of impeller back and housing wall is the same) and an averaged friction coefficient $c_{f,d}$ the specific power loss is

$$h_d = \frac{\pi}{1280} \rho c_{f,d} \Omega^3 D^5 \frac{1}{\dot{m}} . \quad (35)$$

Dividing through $u^2/2$ we get the dimensionless specific power loss due to disc friction

$$\lambda_d = \frac{1}{40} c_{f,d} \frac{1}{\varphi} . \quad (36)$$

Scaling formula. Both the disc friction power λ_d , which increases the necessary shaft power, and the leakage power λ_l has to be considered in the drag coefficient c_d as a power loss, too. Inserting Eq. 32 and the total derivative of Eq. 36 in Eq. 16 we end up with

$$\frac{d\varepsilon}{\varepsilon} = \frac{dc_f}{c_d} + \frac{1}{\varphi} 4\mu d_s \psi^{\frac{3}{2}} \left[\frac{ds}{c_d} - \frac{ds}{\lambda} \right] + \frac{1}{\varphi} \frac{1}{40} \left[\frac{dc_{f,d}}{c_d} - \frac{dc_{f,d}}{\lambda} \right]. \quad (37)$$

As usually $\lambda \gg c_d$ this leads to

$$\frac{ds}{c_d} \gg \frac{ds}{\lambda}, \quad \frac{dc_{f,d}}{c_d} \gg \frac{dc_{f,d}}{\lambda}. \quad (38)$$

and

$$\frac{d\varepsilon}{\varepsilon} = \frac{dc_f}{c_d} + \frac{1}{\varphi} \left[4\mu d_s \psi^{\frac{3}{2}} \frac{ds}{c_d} + \frac{1}{40} \frac{dc_{f,d}}{c_d} \right]. \quad (39)$$

In fans with very low specific speed the disc friction power can be in the order of magnitude of useable fluid power. By neglecting disc friction in fans with higher specific speed and taking the same assumption as for axial fans $c_i \ll c_f$ leads to the scaling formula for centrifugal fans

$$\frac{d\varepsilon}{\varepsilon} = \frac{dc_f}{c_f} + 4\mu d_s \frac{1}{\varphi} \psi^{\frac{3}{2}} \frac{ds}{\varepsilon \lambda}. \quad (40)$$

References

- [1] Pfeleiderer, C., 1955, "Die Kreiselpumpen für Flüssigkeiten und Gase," Springer, Berlin.
- [2] Mühlemann, E., 1948, "Zur Aufwertung des Wirkungsgrads von Überdruck-Wasserturbinen," Schweizerische Bauzeitung, 66. Jahrg, Schweiz.
- [3] Heß, M., Pelz, P., 2010, "On Reliable Performance Prediction of Axial Turbomachines," ASME Turbo Expo, Glasgow, Great Britain, GT2010-22290, ASME, New York.
- [4] Casey, M., Robinson, C., 2011, "A Unified Correction Method for Reynolds Number, Size and Roughness Effects on the Performance of Compressors," Proceedings of the Institution of Mechanical Engineers, Part A: Journal of Power and Energy, Vol. 225, No. 7, pp. 864-876.
- [5] Spurk, J., 1992, "Dimensionsanalyse in der Strömungslehre," Springer, Berlin.
- [6] Pelz, P., Stonjek, S., 2012, "The Influence of Reynolds Number and Roughness on the Efficiency of Axial and Centrifugal Fans – A Physically Based Scaling Method," International Conference on Fan Noise, Technology and Numerical Methods, Fan 2012, 18-20 April 2012, Senlis, France.
- [7] Nakhjiri, M., Pelz, P., Matyschok, B., 2012, "Apparent and Real Efficiency of Turbochargers under Influence of Heat Flow," Isromac-14, 27.02.-02.03.2012, Honolulu, Hawaii.
- [8] Nakhjiri, M., Pelz, P., 2012, "Turbomachines under Periodic Admission – Axiomatic Performance Prediction," In: ASME Turbo Expo 2012, Copenhagen, Denmark, GT2012-68398, ASME, New York.
- [9] Pelz, P., Karstadt, S., 2012, "Tip Clearance Losses - A Physical Based Scaling Method," International Journal of Fluid Machinery and Systems (IJFMS), Vol. 3, pp. 279-284.
- [10] Miller, D., Bailey, A., 1979, "Sphere drag at Mach Numbers from 0.3 to 2.0 at Reynolds Numbers approaching 10^7 ," Journal of Fluid Mechanics, Vol. 93, Part 3, pp. 449-464, Cambridge University Press, Great Britain.
- [11] Schlichting, H., 2005, "Grenzschicht-Theorie," 10th ed, Springer, Berlin.
- [12] Heß, M., 2010, "Aufwertung bei Axialventilatoren – Einfluss von Reynolds-Zahl, Rauheit, Spalt und Betriebspunkt auf Wirkungsgrad und Druckziffer," Ph. D. Thesis, Chair of Fluid Systems Technology, Technische Universität Darmstadt, Germany.
- [13] Schlichting, H., Scholz, N., 1950, "Über die theoretische Berechnung der Strömungsverluste eines ebenen Schaufelgitters," Ingenieur-Archiv.
- [14] Stonjek, S., 2010, "Vorbereitende Arbeiten zur Wirkungsgradaufwertung an Radialventilatoren," Report for the Forschungsgemeinschaft für Luft- und Trocknungstechnik, FLT, Frankfurt a. M.
- [15] Münch, A., 1999, "Untersuchungen zum Wirkungsgradpotential von Kreiselpumpen," Ph. D. Thesis, Fachgebiet für Turbomaschinen und Fluidantriebe, Technische Universität Darmstadt, Germany.
- [16] Tamm, A., 2002, "Beitrag zur Bestimmung der Wirkungsgrade einer Kreiselpumpe durch theoretische, numerische und experimentelle Untersuchungen," Ph. D. Thesis, Fachgebiet für Turbomaschinen und Fluidantriebe, Technische Universität Darmstadt, Germany, 2002.
- [17] DIN EN ISO 5801:2008, "Industrial Fans – Performance Testing Using Standardized Airways (ISO 5801:2007, including Cor 1:2008)," German version EN ISO 5801:2008.
- [18] Hergt, P., Brodersen, S., Stoffel, B., et al., 1995, "The Influence of Prerotation on the Leakage Flow through Sealing Gaps in Pumps," Second International Conference on Pumps and Fans, 17-20 Oct 1995, Beijing, China, pp. 441-449.